Springer

KSME

Journal of Mechanical Science and Technology 24 (2010) 399~406
www.springerlink.com/content/1738-494x
DOI 10.1007/s12206-009-1201-y

Effect of boost pressure on thermal stratification in HCCI engine using the multi-zone model †

O Seok Kwon[1] and Ock Taeck Lim[2]

[1]*Graduate School of Mechanical and Automotive Engineering, Ulsan University Mugeo-dong, Nam-gu, Ulsan 680-749 Korea*
[2]*Department of Mechanical and Automotive Engineering, Ulsan University, Mugeo-dong, Nam-gu, Ulsan 680-749 Korea*

(Manuscript received September 29, 2008; revised July 19, 2009; accepted September 2, 2009)

Abstract

The homogeneous charge compression ignition (HCCI) engine is a next-generation engine offering high efficiency and low emissions. However, the rate of pressure rise is a major limitation for a high load range. Recently, the rate of pressure rise was reduced using thermal stratification. Nevertheless, this was insufficient to produce high power. In the absence of a higher equivalent ratio, one way to improve power is to increase intake boost pressure. The rate of pressure rise is suggested to be reduced by thermal stratification, and power is increased by boost pressure at the same time. The objective of this work is to understand the characteristics of combustion, knock, and emissions for utilizing both thermal stratification and boost pressure. Calculations are performed by CHEMKIN and modified SENKIN. As a result of increasing boost pressure, a higher indicated mean effective pressure (IMEP) was attained, while the rate of pressure rise increased only slightly in HCCI with thermal stratification.

Keywords: HCCI; Rate of pressure rise; Knocking; IMEP; Ringing intensity; Thermal stratification; Multi-zone model; Single-zone model; DME

1. Introduction

To compete with high oil prices and help mitigate the global warming problem, developing a high-efficiency and low-emission engine is essential. The homogeneous charge compression ignition (HCCI) engine, which ignites a homogeneous charge by compression of the piston, is a promising candidate. An HCCI engine produces low particulate matter (PM) and nitrogen oxide (NOx) emissions by using an ultra-lean premixture, offering high efficiency owing to a high compression ratio similar to that of the compression ignition (CI) engine.

However, despite these advantages, the use of HCCI engines has not been realized. This is primarily due to the knocking associated with an excessive rate of pressure rise at high–load operations during combustion. To address this concern, recent reports have suggested reducing the rate of pressure rise by thermal stratification, fuel stratification, and combustion retard [1-3].

For thermal stratification, the local gas temperature difference affects combustion phasing. Therefore, continuous combustion reduces the rate of pressure rise, and a higher initial temperature and wider thermal width help decrease it. Nevertheless, an HCCI engine is insufficient in producing high power.

In the absence of a higher equivalent ratio, one way to improve power is to increase intake boost pressure [4-6]. The effect of boost pressure is that as the booster increases an initial pressure, air density increases. Although the equivalent ratio remains constant, power can be increased by intensifying a heat input unit cycle.

An existing study merely focuses on thermal stratification for reducing the rate of pressure rise in HCCI combustion. In this study, it is suggested that the rate of pressure rise is reduced by thermal stratification, and power is increased by boost pressure simultaneously. The objective of this work is to understand the characteristics of combustion, knock, and emissions for utilizing both thermal stratification and boost pressure.

Di-methyl ether (DME), which is characterized by low temperature reaction (LTR) and high temperature reaction, was utilized as test fuel. DME produces high heat release during LTR, so a significant temperature difference exists immediately before HTR. Thus, DME is more appropriate for producing thermal stratification by heat release in LTR. The characteristics of DME compared to n-Butane and iso-Octane are outlined in Table 1.

† This paper was recommended for publication in revised form by Associate Editor Kyoung Doug Min

*Corresponding author. Tel.: +82 52 259 2852, Fax.: +82 52 259 1680
E-mail address: otlim@ulsan.ac.kr

Table 1. Fuel properties.

Name	DME	n-Butane	Iso-Octane
Molecular formula	CH_3OCH_3	C_4H_{10}	C_8H_{18}
Lower heating value (kcal/m^3)	14,143	26,504	47,832
Cetane number	55-60	<10	<10
Low-temperature reaction (%)	10-30	0-5	0-5
Hig-temperature reaction (%)	70-90	95-100	95-100

Table 2. Engine specification.

Displacement [cc]	1133
Bore (mm)	112
Stroke (mm)	115
Connecting Rod Length (mm)	205
Compression Ratio	21.6
Number of Valves	2
IVC (deg ABDC)	48
EVO (deg ABDC)	312

2. Calculation method

In this study, CHEMKIN2 and modified SENKIN, software programs developed at Sandia National Laboratories, are utilized from homogeneous temperature to thermal stratification conditions [7, 8]. Curran`s scheme (species: 78, reaction: 336) is utilized as the chemical reaction model of DME [9] Table 2 shows the specifications of the engine as a yammer single cylinder, which is used for the calculation.

A range of calculation is from right after intake valve close to right before exhaust valve open. The thermodynamic characteristics of gas are calculated in merely one compression and expansion stroke. It is assumed that all gas is ideal gas (1), and heat and mass transfer are not considered.

Two conservation laws are observed: The energy conservation law (2) and the mass conservation law (3). In one zone, the gas pressure, temperature, and composition of species are completely uniform. In-cylinder mass average gas temperature $\overline{T_c}$ is calculated with total energy equation (4).

$$Pv = nRT \tag{1}$$

$$C_v \frac{dT}{dt} + P\frac{dv}{dt} + q_{REAC} = 0 \tag{2}$$

$$\frac{dm}{dt} = 0 \tag{3}$$

$$\overline{T_c} = \frac{\sum_{i=1}^{N}(n_i \cdot c_{p,i} \cdot T_{c,i})}{\sum_{i=1}^{N}(n_i \cdot c_{p,i})} \tag{4}$$

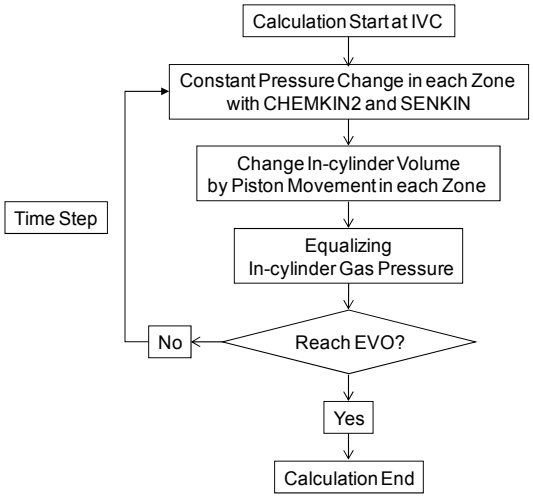

Fig. 1. Algorithm flow diagram for the multi-zone model.

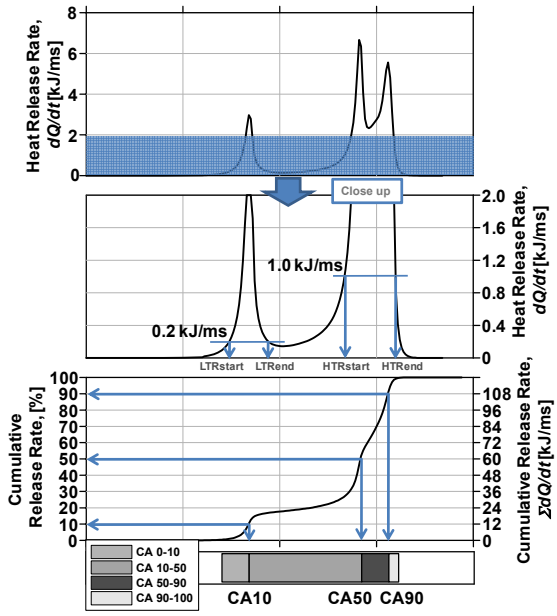

Fig. 2. Definition of combustion duration.

where

N: Number of zone

n_i: Number of moles

$C_{p,i}$: Specific heat at a constant pressure of i_{th} zone

As the initial pressure increases, a heat input per cycle Q_{in} (5) is calculated as

$$Q_{in} = \sum_{i=1}^{N} n_i \cdot (Q_{LHV} \cdot \frac{FA_i}{1 + FA_i}) \tag{5}$$

where

Q_{LHV}: Low heat value of DME

FA_i: Volume ratio of fuel to air of i_{th} zone

Heat transfer and blow-off were not taken into account in the calculation. Each zone of the multi-zone area for thermal stratification was based on a single zone model for homogeneous temperatures. Fig. 1 demonstrates the process of multi-zone calculation. After inputting the initial pressure, temperature, and volume, the pressure of each zone increased regularly, and the volume of each was altered by the piston compression after the right intake valve closed. The amount of volume change of each zone was again converted to pressure, which was equilibrated. The equilibrated pressure was substituted by the next pressure value.

As Fig. 2 illustrates, combustion duration was defined by the starting point and end point of LTR, which were heat release rate=0.2 kJ/ms, and the starting point and end point of HTR, which were heat release rate=1.0 kJ/ms. However, the boundary between LTR and HTR was indistinct in thermal stratification. Thus, for thermal stratification, combustion duration was defined by the position of 10%, 50%, and 90% burn point of total heat release - CA10, CA50, and CA90, respectively.

The most elementary knocking criterion employed to limit the allowable operating range without knocking HCCI combustion was to specify a limit on the maximum rate of cylinder pressure rise. Although setting the limit of the maximum rate of pressure rise is a useful metric, it does not appear to be a uniformly appropriate criterion [10]. For example, Christensen et al. operated an HCCI engine under both naturally aspirated and supercharged conditions. They reported that a larger maximum rate of pressure rise could be withstood for supercharged conditions without knocking (an undue increase in engine noise) than for the naturally aspirated system. The ringing intensity (RI) developed by J.A. Eng was employed to confirm the occurrence of knocking [10]. In this work, knocking was confirmed and identified by RI. Therefore, 5 MW/m^2 was selected as the limit for an acceptable RI in the HCCI engine [15].

$$RI = \frac{1}{2\gamma} \times \frac{(0.05 \times (\frac{dp}{dt})_{\max})^2}{P_{\max}} \times \sqrt{\gamma R T_{\max}} \quad (6)$$

where

dt_{max}= maximum pressure rise rate
P_{max}: maximum pressure
T_{max}: maximum temperature
γ: C_p/C_v
R: gas constant of air

3. Calculation Results

3.1 Homogeneous Temperature

3.1.1 Characteristics of HCCI combustion by increasing initial temperature

Fig. 3 illustrates the traces of pressure, temperature, and heat release at initial temperatures of 293, 353, 413, and 473 K.

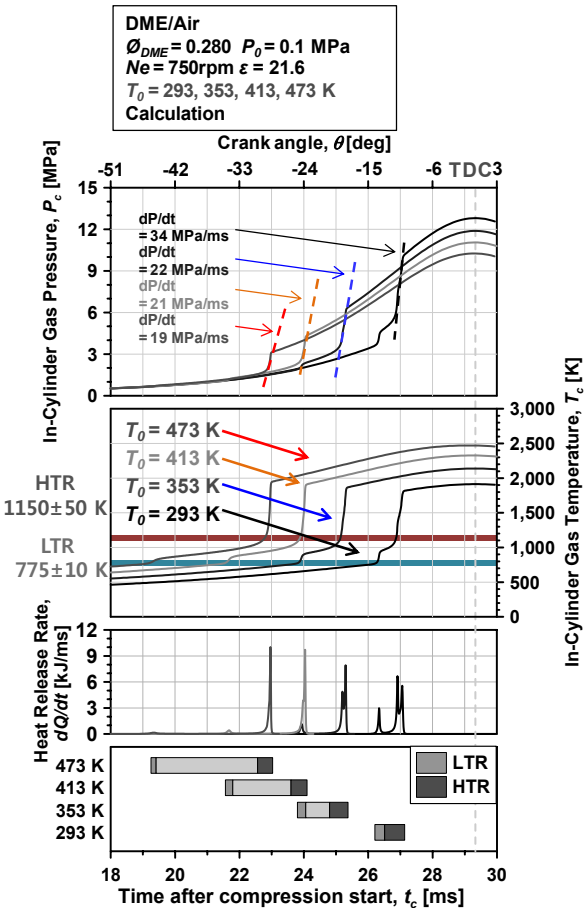

Fig. 3. History of pressure, temperature, heat release rate, and combustion duration at T_0=293, 353, 413, and 473, P_0=0.1 MPa.

The rate of pressure rise was approximately 19, 21, 22, and 34 MPa/ms, and the maximum pressure was 10, 11, 12, and 13 MPa at initial temperatures of 293, 353, 413, and 473 K, respectively. As the initial temperature increased, the rate of pressure rise and maximum pressure decreased. In general, as the initial temperature increases, final state parameters such as pressure and temperature are increased. In this case, CA50 occurs after TDC. Heat of combustion accompanies pressure rise. Thus, there is maximum pressure given the condition that CA50 occurs near TDC.

When the initial temperature increased from 273 to 473 K, the maximum temperature increased from 1,913 to 2,472 K. Independent of initial temperature, both LTR and HTR started at 775 ± 10 and 1,150 ± 50 K, respectively. Maximum heat release rate increased, but the heat release rate at LTR decreased as the initial temperature increased. Total combustion duration decreased, and both LTR and HTR advanced as initial temperature increased.

If the thermal stratification effect exists in the in-cylinder (if initial temperature of each zone is different), ignition occurs in sequence from a high-temperature to a low-temperature region. Thus, the time of maximum heat release may occur in sequence. It is expected that the maximum rate of pressure rise would decrease.

3.1.2 Characteristics of HCCI combustion by increasing initial pressure

Fig. 4 illustrates the trace of pressure and temperature at an initial temperature of 383 K and an initial pressure of 0.1, 0.12, 0.14, 0.16, and 0.18 MPa as homogeneous temperature. Heat addition was 848, 1,004, 1,171, 1,339, and 1,506 J/cycle at an initial pressure of 0.1, 0.12, 0.14, 0.16, and 0.18 MPa, respectively. When the initial pressure changed from 0.1 to 0.18 MPa, the maximum pressure increased from 11 to 21 MPa—a difference of approximately 10 MPa. Further, the maximum temperature increased to approximately 54 K from 2,236 to 2,290 K. Changing the initial pressure created an effect on maximum pressure, but it posed a negligible effect on maximum temperature.

Fig. 5 presents the combustion duration (t = 22 ~ 25 ms). The initial pressure increased from 0.1 to 0.18 MPa, and the maximum rate of pressure rise was 22.1, 21.9, 21.4, and 23.1 MPa/ms. Changing the initial pressure did not significantly affect the rate maximum pressure rise for the combustion duration. Independent of initial pressure, both LTR and HTR occurred at a regular temperature: 780 ± 10 K and 1110 ± 30 K, respectively. The heat release rates at both HTR and LTR increased as initial pressure increased. When the initial pressure increased from 0.1 to 0.18 MPa, two spikes of HTR were observed. If the initial pressure increased from 0.1 to 0.18 MPa, then LTR and HTR advanced by 0.17 and 0.98 ms, respectively. The combustion duration was approximately 2.04 and 1.27 ms when the initial pressure was 0.1 MPa and 0.18 MPa, respectively. Combustion duration was reduced by approximately 0.77 ms. The total combustion duration was reduced as initial pressure increased.

3.1.3 Chemical species concentration profile

The chemical species concentration profile (Figs. 6-9) demonstrates the mole fraction histories of chemical species at various initial temperatures and pressures. These figures include the history of pressure, temperature, and heat release for each condition. At the time of heat release, DME (CH_3OCH_3) begins to reduce, and concentrations of CO, CO_2, HCHO, and H_2O_2 increase rapidly. Concentrations of HCHO and H_2O_2 affecting the HTR begin to decrease quickly at the start of HTR. The behavior of OH mole fraction has the same tendency as the heat release rate [11]. HTR rises by the activation of the decomposition reaction of H_2O_2 accumulated in LTR to OH [12].

The mole fraction histories of each chemical species at an initial temperature of 293 and 473 K are outlined in Figs. 6- 7. Concentrations of H_2O_2 and HCHO lasted from the beginning of LTR to the end of HTR. As the initial temperature increased from 293 to 473 K, they remained at a peak value, at approximately 0.63 and 3.61 ms, respectively. As the initial temperature was high, both HCHO and H_2O_2 were consumed slowly. An existing period of intermediates increased to approximately 2.98 ms when the initial temperature increased from 273 to 473 K. As a result, it was observed that the maximum rate of pressure rise decreased.

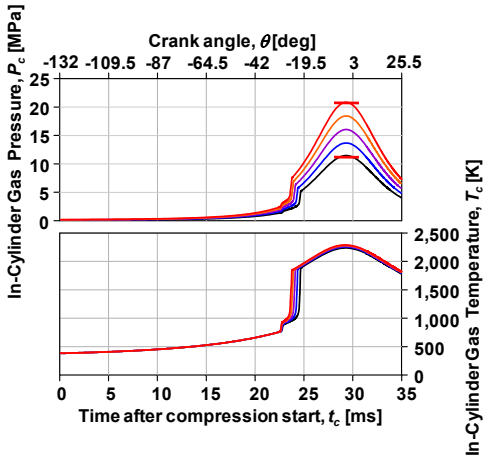

Fig. 4. History of pressure and temperature at T_0=383K, P_0=0.1, 0.12, 0.14, 0.16, and 0.18MPa.

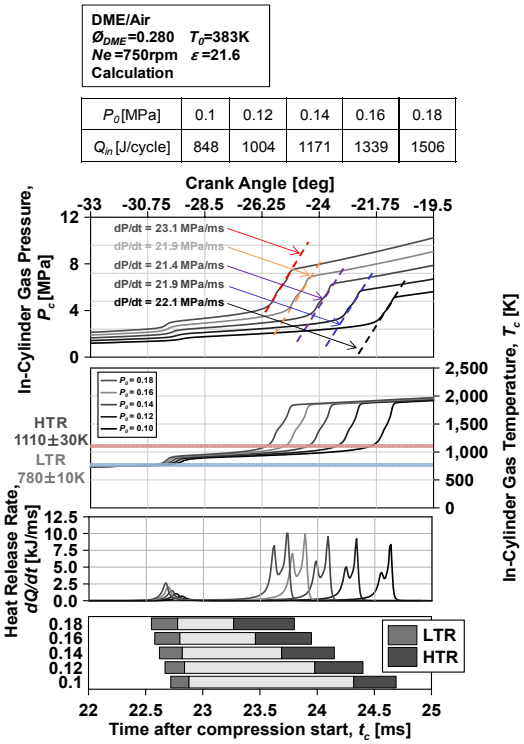

Fig. 5. History of pressure, temperature, and heat release rate at T_0=383K, P_0=0.1, 0.12, 0.14, 0.16, and 0.18MPa.

The mole fraction histories of each chemical species at an initial pressure of 0.1 and 0.18 MPa are presented in Figs. 8-9. Concentrations of H_2O_2 and HCHO lasted from the beginning of LTR to the end of HTR.

As the initial pressure increased from 0.1 to 0.18 MPa, they

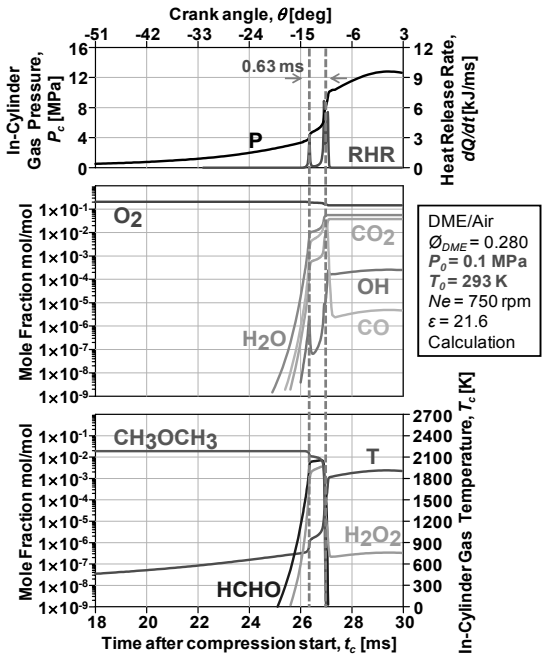

Fig. 6. Radical history at an initial temperature of 293K under homogeneous temperature condition.

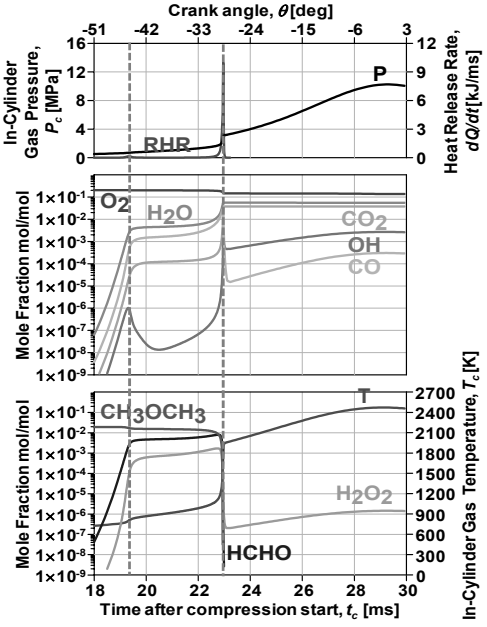

Fig. 7. Radical history at an initial temperature of 473K under homogeneous temperature condition.

remained at a peak value, at approximately 1.76 and 0.96 ms, respectively. An existing period of intermediates decreased at approximately 0.8 ms when the initial pressure increased from 0.1 to 0.18 MPa. As initial pressure was high, an existing period of intermediates decreased. When the initial pressure increased from 0.1 to 0.18 MPa despite the increase in heat input, the mole fraction of H_2O_2, which affected HTR, remained nearly between LTR and HTR. Thus, the rate of pressure rise did not increase significantly, possessing a similar value.

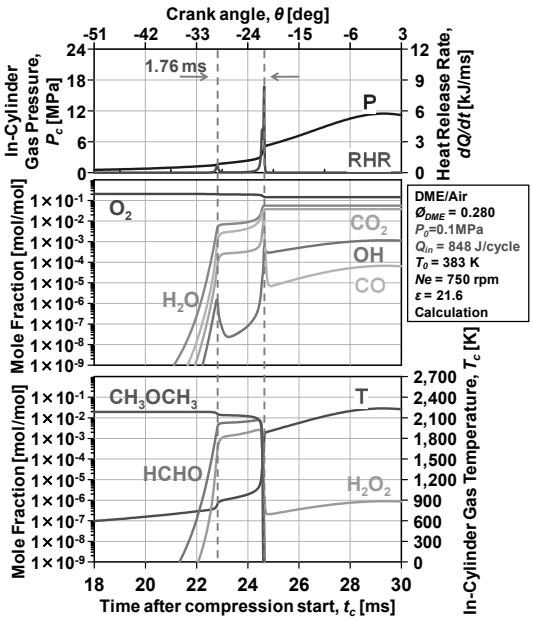

Fig. 8. Radical history at an initial pressure of 0.1MPa under homogeneous temperature condition.

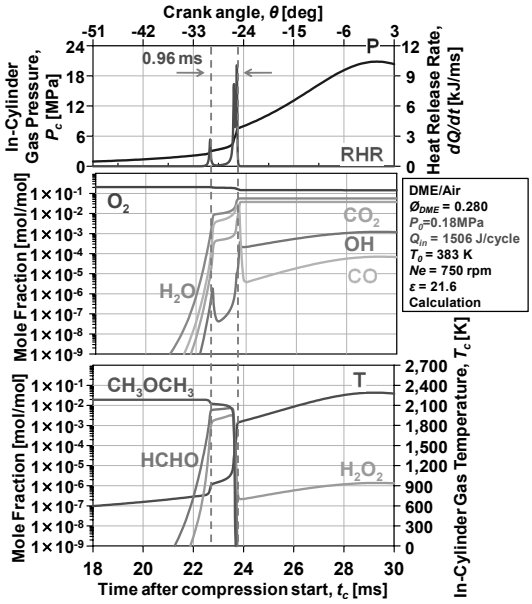

Fig. 9. Radical history at an initial pressure of 0.18MPa under homogeneous temperature condition.

3.2 Thermal stratification

3.2.1 Characteristics of HCCI combustion by increasing booster pressure

Fig. 10 displays the traces of pressure, temperature, and rate of heat release when the initial average temperature was $\overline{T_0}$ = 383 K, the thermal width was TW = 100 K, and the initial pressure was P_0 = 0.1, 0.12, 0.14, 0.16, and 0.18 MPa. Heat addition was 855, 1012, 1181, 1350, and 1519 J/cycle at an initial pressure of 0.1, 0.12, 0.14, 0.16, and 0.18 MPa, respectively. The maximum pressure increased from 12 to 21 MPa

when the initial pressure was modified from 0.1 to 0.18 MPa—a difference of approximately 9 MPa. Further, the maximum temperature increased approximately 49 K from 2,236 to 2,285 K. Similar to the homogeneous temperature condition, changing the initial pressure had an effect on maximum pressure but posed a negligible effect on maximum temperature under thermal stratification.

Combustion duration (t = 20-26ms) is presented in Fig. 11. The maximum rate of pressure rise increased by approximately 3.5 MPa/ms from 4.4 to 7.9 MPa/ms when initial pressure increased from 0.1 to 0.18 MPa. As compared to homogeneous temperature, the maximum rate of pressure rise was reduced significantly by thermal stratification. Both LTR and HTR were clearly differentiated at a homogeneous temperature; however, the boundary between LTR and HTR was indistinct in thermal stratification. Therefore, as Fig. 2 illustrates, combustion duration was applied. CA10 and CA50 increased by 1.04 ms and 0.94 ms, respectively, as initial pressure increased from 0.1 to 0.18 MPa. Additionally, the duration of the period during which heat was significantly emitted, CA10-90, was 1.3 and 1.43 ms with an initial pressure of 0.1 and 0.18 MPa, respectively. It was confirmed that total combustion duration decreased. In contrast, CA10-90 increased when the initial pressure increased.

3.3 Ringing intensity and IMEP

Fig. 12 presents the effect of increasing the initial pressure on RI and IMEP under thermal stratification. All cases have the equivalent ratio $Ø_{DME}$ = 0.280 and initial pressure of P_0 = 0.1, 0.12, 0.14, 0.16, and 0.18 MPa. For thermal stratification, the initial average gas temperature $\overline{T_0}$ =383 K and thermal width TW = 100 K. Meanwhile, for homogeneous temperature, initial gas temperature T_0 = 383 K and thermal width TW = 0 K.

3.3.1 For homogeneous temperature

As initial pressure increased, RI decreased from 36.01 to 21.92 MW/m^2, a difference of approximately 14.09 MW/m^2. Meanwhile, IMEP increased from 0.493 to 0.818 MPa, a difference of approximately 0.325 MPa.

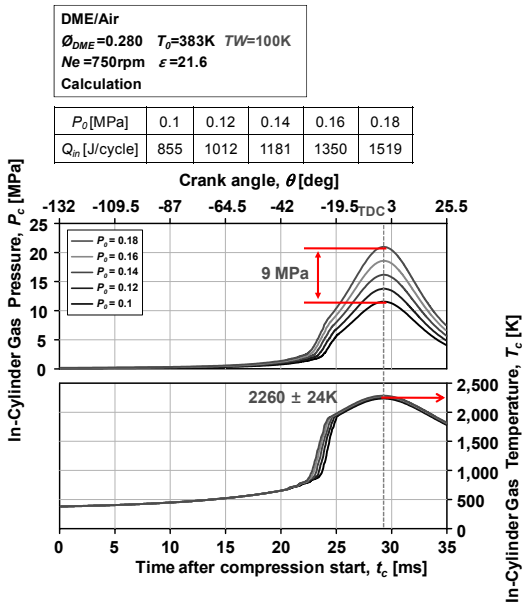

Fig. 10. History of pressure and temperature under thermal stratification condition.

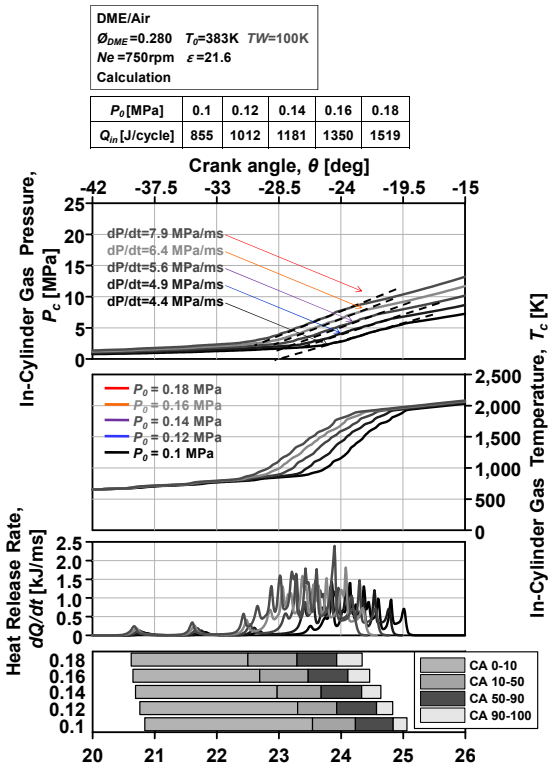

Fig. 11. History of pressure, temperature, and heat release rate under thermal stratification condition.

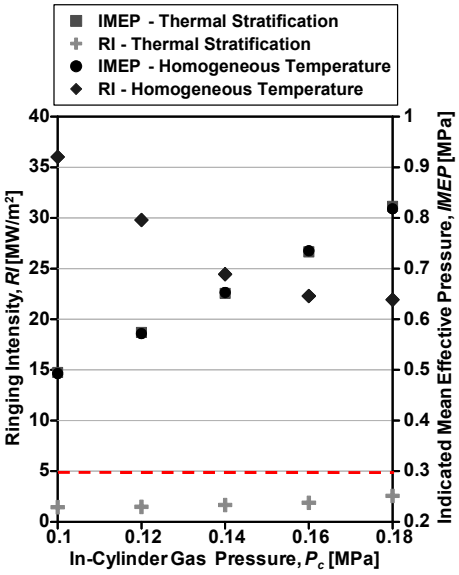

Fig. 12. RI and IMEP at initial pressure of 0.1, 0.12, 0.14, 0.16, and 0.18 MPa under thermal stratification and homogeneous temperature.

3.3.2 For thermal stratification

As initial pressure increased, RI increased from 1.44 to 2.56 MPa, a difference of approximately 1.12 MW/m^2. RI appeared to be under 5 MW/m^2 (a range within which knocking can be avoided). IMEP increased from 0.491 to 0.807 MPa, a difference of approximately 0.316 MPa. Thermal stratification did not affect IMEP. Therefore, IMEP under thermal stratification case is similar to that under a homogeneous temperature case. Though the equivalent ratio remained constant, IMEP was increased by growing a heat input per unit cycle.

3.4 Emission of HCCI combustion

Fig. 13 presents the traces of temperature, IMEP, and emissions of CO and NOx for homogeneous temperature conditions, thermal stratification conditions (P_0 = 0.1 MPa, TW = 100 K), and both thermal stratification and booster (P_0 = 0.18 MPa, TW = 100 K) conditions when RI was approximately 5 MW/m^2 to avoid knocking.

The first case was for a homogeneous temperature, with the following values: equivalent ratio, $\emptyset_{DME}$ = 0.22; initial pressure, P_0 = 0.1 MPa; initial temperature, T_0 = 383 K; and heat input, Q_{in} = 669 J/cycle.

The second case was for thermal stratification only, with the following values: equivalent ratio, $\emptyset_{DME}$ = 0.35; initial pressure, P_0 = 0.1 MPa; initial average gas temperature, $\overline{T_0}$ = 383 K; thermal width, TW =100 K; and heat input, Q_{in} = 1064 J/cycle.

The third case was for both the thermal stratification and booster, with the following values: equivalent ratio, $\emptyset_{DME}$ = 0.35; initial pressure, P_0 = 0.18 MPa; initial average gas temperature, $\overline{T_0}$ = 383 K; thermal width, TW = 100 K; and heat input, Q_{in} = 1889 J/cycle.

3.4.1 For a homogeneous temperature vs. for thermal stratification only

IMEP increased from 0.407 to 0.576 MPa, and maximum temperature increased from 2,019 to 2,454 K because the equivalent ratio increased from 0.22 to 0.35. CO emission when $\emptyset_{DME}$= 0.22 decreased as compared to that observed when $\emptyset_{DME}$= 0.35. CO was considerably generated in the presence of insufficient oxygen to convert all carbon to CO_2 and when an engine ran rich [13]. It appeared that NO_x emission when $\emptyset_{DME}$= 0.22 was similar to that when $\emptyset_{DME}$= 0.35.

3.4.2 For thermal stratification only vs. for thermal stratification and boost pressure

Without regard to the change in initial pressure, it appeared that the maximum in-cylinder gas temperature was similar.

The CO emission when the initial pressure was 0.18 MPa decreased approximately 55% more than when the initial pressure was 0.1 MPa. As initial pressure increased to 0.18 MPa, air density increased as well. Hence, volume efficiency improved, and carbon monoxide was decreased [13].

The NOx emission when the initial pressure was 0.18 MPa

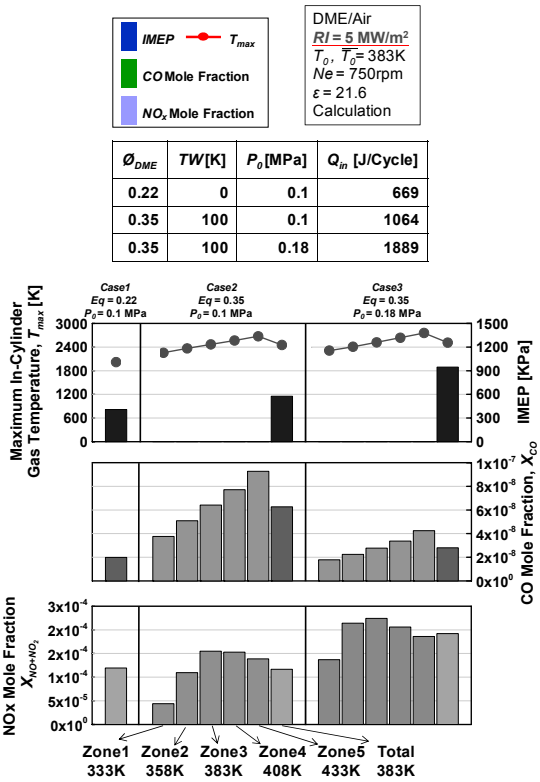

$\emptyset_{DME}$	TW[K]	P_0[MPa]	Q_{in} [J/Cycle]
0.22	0	0.1	669
0.35	100	0.1	1064
0.35	100	0.18	1889

Fig. 13. IMEP, maximum gas temperature, and CO and NOx emissions under RI ≤ 5MW/m^2.

increased approximately 65% greater as compared to that for a case wherein the initial pressure was 0.1 MPa. Significant NOx was generated when the combustion temperature was greater than 2200 K. [14] In addition to temperature, the formation of NOx depends on the pressure, air-fuel ratio, and combustion time within the cylinder, chemical reactions not being instantaneous [13]. The period during which the in-cylinder gas temperature remained greater than 2,200 K was 8.54 and 7.48 ms for an initial pressure of 0.18 MPa and 0.1 MPa, respectively [Appendix A]. Despite a different initial pressure, the in-cylinder gas temperature remained similar. However, because the period in which the in-cylinder gas temperature remained greater than 2,200 K increased as initial pressure increased, the rate of NOx emission increased as well.

4. Conclusion

The objective of this work is to understand the characteristics of combustion, knock, and emissions for use in both thermal stratification and boost pressure.

The following results were obtained from this work:

- For a homogeneous temperature:

As the initial temperature increased, the maximum rate of pressure rise decreased. Both LTR and HTR advanced, and combustion duration increased.

As initial temperature increased, both HCHO and H_2O_2 were consumed slowly. An existing period of intermediates

increased to allow the maximum rate of pressure rise to decrease.

As initial pressure increased despite the increase in maximum pressure, the maximum temperature remained constant. Both LTR and HTR advanced, and the combustion duration decreased.

When the initial pressure increased from 0.1 to 0.18 MPa despite the increase in heat input, the mole fraction of H_2O_2, which affected HTR, remained nearly between LTR and HTR. Thus, the rate of pressure rise did not increase significantly.

- For thermal stratification:

Both maximum pressure and temperature were similar to the case involving homogeneous temperature. However, the maximum rate of pressure rise and RI decreased by thermal stratification.

Although the equivalent ratio is the same as the initial pressure increased, IMEP was increased by growing the heat input unit cycle.

As the initial pressure increased, air density increased as well, and volume efficiency improved. Hence, the rate of CO emission decreased.

The period during which the in-cylinder gas temperature remained greater than 2,200 K increased as the initial pressure increased, so the rate of NOx emission increased significantly as well.

Acknowledgement

This work was supported by the development program of the local science park funded by the ULSAN Metropolitan City and the Ministry of Education, Science and Technology (MEST).

References

[1] M. Sjoberg, J. E. Dec and N. P. Cernansky, Potential of thermal stratification and combustion retard for reducing pressure-rise rates in hcci engines, based on multi-zone modeling and experiments, *SAE (*2005) 2005-01-0113.

[2] J. Ozaki and N. Iida, Effect of degree of unmixedness on HCCI combustion based on experiment and numerical analysis, *SAE* (2006) 2006-32-0046.

[3] D. Yamashita, S. Kweon, S. Sato and N. Iida, The study on auto-ignition and combustion process of the fuel blended with methane and DME in HCCI engines, *Transaction of JSAE* 36 (6) (2005) 85-90.

[4] M. Christensen and B. Johansson, Supercharged homogeneous charge compression ignition (HCCI) with exhaust gas recirculation and pilot fuel, *SAE* (2000) 2000-01-1835.

[5] M. Christensen, B. Johansson, P. Amneus and F. Mauss, Supercharged homogeneous charge compression ignition, *SAE* (1998) 980787.

[6] E. J. Silke, W. J. Pitz and C. K. Westbrook, Understanding the chemical effects of increased boost pressure under HCCI conditions, *SAE* (2008) 2008-01-0019.

[7] A. E. Luz, F. Rupley and J. A Miller, CHEMKIN-II:A FORTRAN chemical kinetics pacage for the analysis of gas-phase chemical kinetics, *Sandia National Laboratories Report, SAND* (1989) 89-8009B.

[8] A. E. Luz, R. J. Kee and J. A. Miller, SENKIN: A FORTRAN program for predicting homogeneous gas phase chemical kinetics with sensitivity analysis, *Sandia National Laboratories Report, SAND (*1988)87-8248.

[9] H. J. Curran, W. J. Pitz, C. K. Westbrook, P. B. Dagaut, J-C Boettner and M. Cathonnet, A wide range modeling study of dimethyl ether oxidation, *International Journal Chemical Kinetics,* 30 (3) (1998), 229-241.

[10] J. A. Eng, Characterization of pressure waves in hcci combustion, *SAE* (2002) 2002-01-2859.

[11] S. Sato and N. Iida, Analysis of DME homogeneous charge compression ignition combustion, *SAE* (2003) 2003-01-1825.

[12] H. Yamada, Y. Goto and A. Tezaki, Analysis of reaction mechanisms controlling cool and thermal flame with DME fueled HCCI engines, *SAE* (2006) 2006-01-3299.

[13] W. W. Pulkrabek, Engineering fundamentals of the internal combustion engine, *Pearson Prentice Hall*, (1997).

[14] K. Akihama, Y. Takatori, K. Inagaki, S. Sasaki and A. M. Dean, Mechanism of the smokeless rich diesel combustion by reducing temperature, *SAE* (2001) 2001-01-0655.

[15] M. Sjöberg, J. E. Dec, A. Babajimopoulos and D. Assanis, Comparing enhanced natural thermal stratification against retarded combustion phasing for smoothing of HCCI heat-release rates, *SAE* (2004) 2004-01-2994.

Ock-Taeck Lim received his B.S. and M.S. degrees in Mechanical Engineering from Chonnam National University, Korea, in 1998 and 2002, respectively. He then received his Ph.D. degree from Keio University in 2006. Dr. Lim is currently a professor at the School of Automotive and Mechanical Engineering at Ulsan University in Ulsan, Korea. His research interests include internal combustion engines, alternative fuel, and thermodynamics.